ANALYSIS OF THE DIFFUSE IONIZED GAS DATABASE: DIGEDA

Nahiely Flores-Fajardo, Christophe Morisset, and Luc Binette

Instituto de Astronomía, Universidad Nacional Autónoma de México, Mexico

RESUMEN

Los estudios del Gas Ionizado Difuso (DIG), hasta el momento se han hecho sin un consenso del criterio estricto para diferenciar entre el DIG y las regiones H II. En este trabajo recopilamos las mediciones de las líneas en emisión de 29 galaxias disponibles en la literatura, creando la primera base de datos del DIG (DIGEDA). Haciendo uso de esta base, analizamos las propiedades globales del DIG a partir de los cocientes de líneas [N II]λ6583/Hα, [O I]λ6300/Hα, [O III]λ5007/Hβ y [S II]λ6716/Hα, así como la medida de emisión de Hα. Este análisis nos permitió concluir que el cociente [N II]/Hα es un criterio general para diferenciar si una región en emisión es DIG o región H II, mientras que la EM(Hα) es una cantidad útil únicamente cuando consideramos galaxias por separado. Finalmente, encontramos que las regiones clasificadas como DIG en galaxias Irr parecen tener un comportamiento más cercano al de las regiones H II que al DIG en galaxias espirales.

ABSTRACT

Studies of the Diffuse Ionized Gas (DIG) have progressed without providing so far any strict criterion to distinguish DIGs from H II regions. In this work, we compile the emission line measurements of 29 galaxies that are available in the scientific literature, thereby setting up the first DIG database (DIGEDA). Making use of this database, we proceed to analyze the global properties of the DIG using the [N II]λ6583/Hα, [O I]λ6300/Hα, [O III]λ5007/Hβ and [S II]λ6716/Hα lines ratios, including the Hα emission measure. This analysis leads us to conclude that the [N II]/Hα ratio provides an objective criterion for distinguishing whether an emission region is a DIG or an H II region, while the EM(Hα) is a useful quantity only when the galaxies are considered individually. Finally, we find that the emission regions of Irr galaxies classified as DIG in the literature appear in fact to be much more similar to H II regions than to the DIGs of spiral galaxies.

Key Words: astronomical data bases: miscellaneous — galaxies: general — ISM: HII regions — ISM: lines and bands — line: formation

1. INTRODUCTION

From observations of free-free continuum absorption, Hoyle & Ellis (1963) inferred the existence of a new gas component of the interstellar medium (ISM). They proposed that this new component was warm ($T_e \sim 10^4$ K), of low density ($n_e \sim 10^{-1}\,cm^{-3}$), ionized and that it surrounded the Milky Way's disk. The integrated luminosity of this hypothetical medium was comparable to that expected from photoionization by O and B stars from the disk.

The existence of this gas component was later confirmed by the signal dispersion from pulsars and by the detection of faint optical emission lines from the galactic diffuse interstellar medium (Reynolds, Scherb, & Roesler 1973). Deep images of external galaxies such as NGC 891 show a similar warm gas component (Dettmar 1990; Rand 1998). This component has since been found in several other galaxies (e.g., Bland-Hawthorn, Sokolowski, & Cecil 1991a,b; Veilleux, Cecil, & Bland-Hawthorn 1995; Greenawalt, Walterbos, & Braun 1997; Martin & Kennicutt 1997; Wang, Heckman, & Lehnert 1997). Today, it carries various names, such as WIM (Warm Ionized Medium), DIM (Diffuse Ionized Medium), DIG (Diffuse Ionized Gas) or eDIG (extraplanar

DIG), and "Reynold's Layer" (in the case of the Galaxy). Hereafter, we will use the generic names DIG and eDIG.

Despite the fact that the DIG in our Galaxy accounts for $\sim 90\%$ of the ionized medium's mass (Reynolds 1991), the nature of this low density plasma is far from being well understood. The first problem encountered in DIG studies is how to formally distinguish DIGs from H II regions, which similarly consist of a warm and ionized gas phase. Several methods have been proposed in the literature. Examples are the Hα equivalent width (Bland-Hawthorn et al. 1991a), the Hα emission measure[1], EM (e.g., Walterbos & Braun 1994), or the surface brightness (e.g., Ferguson et al. 1996). Nevertheless, none of the methods has so far been accepted as standard, mainly because the density and size of the emitting regions are usually unknown. To illustrate the above problem, an example is provided by the galaxy M31, for which Walterbos & Braun (1994) adopted the EM criterion to distinguish DIGs from H II regions. They found that close to low star formation regions, the DIG always had an EM $< 50\,\mathrm{pc\,cm^{-6}}$, while near higher star formation regions, the latter had an EM near $100\,\mathrm{pc\,cm^{-6}}$. Therefore, even though the EM is proportional to the electron density and should thereby reflect how "diffuse" an emission region is, this criterion was shown to vary with position in this galaxy.

Another problem in the study of the DIG is the difficulty in observing it, mainly because of its low surface brightness. As a result, the observations in the literature are sparse and only a few line ratios are typically reported. Furthermore, systematical comparative studies of the general behavior of the EMs or of line ratios among different objects are still missing. For example, even though a majority of authors agree on the existence of an anti-correlation between the [N II]$\lambda6583$/Hα or [S II]$\lambda6716$/Hα ratios with the EM (these ratios increase when the EM decreases, e.g., Bland-Hawthorn et al. 1991a; Rand 1998), very few studies were done with more than two galaxies (e.g., Wang et al. 1997; Zurita, Rozas, & Beckman 2000; Tüllmann & Dettmar 2000; Miller & Veilleux 2003). In this work, we will verify for the first time whether such an anticorrelation is a general feature of the DIG or not. Another interesting aspect is the apparent confusion concerning the [O III]$\lambda5007$/Hβ ratio in the literature, for which some authors report a constant behavior with EM (e.g., Wang et al. 1997, at least for some galaxies), while others report

an increase when the EM decreases (e.g., Rand 1998; Tüllmann & Dettmar 2000).

The spectral characteristics (different from those of H II regions) combined with the large spatial extension of the DIG (typically $|z| \approx 2$ kpc), are not well reproduced by models that consider only photoionization from O-B stars (e.g., Rand, Wood, & Benjamin 2009), even though it could provide the entire UV photon flux required to mantain the DIG ionized (e.g., Reynolds 1990; Zurita et al. 2000). As a result, several authors have suggested that the DIG could be excited by extra ionization (or heating) sources like: shocks (e.g., Sivan, Stasińska, & Lequeux 1986), mixing layers (e.g., Binette et al. 2009), old hot stars (e.g., Sokolowski & Bland-Hawthorn 1991), and decaying dark matter (e.g., Dettmar & Schultz 1992). In the study of the Seyfert 2 galaxy NGC 1068, Bland-Hawthorn et al. (1991b) proposed photoionization by the AGN power law. None of these models is completely successful in explaining the line ratios, spatial extensions and luminosities of the DIGs in spiral galaxies. For a complete review of the posibles DIG ionizing or heating sources, see Bland-Hawthorn, Freeman, & Quinn (1997).

With the previous arguments in mind, and to correct for the lack of comparative studies in the field of diffuse emission, we have compiled a comprehensive database of emission line ratios or fluxes, from DIGs or H II regions, published in the literature. This database is hereafter called the Diffuse Ionized Gas Emission Database (DIGEDA) which will soon be available at the VizieR website of CDS (Centre de Données Astronomiques de Strasbourg, `http://vizier.u-strasbg.fr`).

The structure of the article is the following: after describing DIGEDA in § 2, we proceed with the analysis and interpretation of the data in § 3. A discussion follows in § 4 and a brief conclusion is given in § 5.

2. THE DIG DATABASE

An extensive research on DIG observations in the literature led us to build a comprehensive database comprising DIG and H II region spectroscopic observations of 29 different galaxies (25 spiral galaxies and 4 irregulars). This survey contains galaxies with a significant spread in star formation rates, Hα luminosities, distances, disk inclinations, slit positions and slit orientations.

2.1. Internal data structure of DIGEDA

Table 1 lists the 17 bibliographic references used in DIGEDA, which amounts to a total of 1061 line

---

[1]The EM in units of $\mathrm{pc\,cm^{-6}}$ is defined as EM $\equiv \int n_e n_{H^+}\,ds \approx \int n_e^2\,ds$.

TABLE 1

BIBLIOGRAPHICAL REFERENCES USED FOR THE COMPILATION OF DIGEDA

Ref_ID[a]	Author	Galaxy	Slit[b]	Observations[c]	No. regions
1	Benvenuti, D'Odorico, & Peimbert (1976)	M33	Interarm	[O III] λ4959, [O III], [N II]	62
2	Golla, Dettmar, & Domgorgen (1996)	NGC 4631	$\perp$	[N II], [S II]	39
			$\parallel$	[N II], [S II]	80
3	Greenawalt et al. (1997)	M31	DIG, H II	[O II], [O III], [N II], [S II]+, EM	18
4	Martin & Kennicutt (1997)	NGC 1569	DIG	[O III], He I, [O I], [N II], [S II]+	25
5	Wang et al. (1997)	M51	Interarm	[O III], [N II], [S II]+	3
		M101	Interarm	[O III], [N II], [S II]+	6
		NGC 2403	Interarm	[O III], [N II], [S II]+	5
		NGC 4395	Interarm	[O III], [N II], [S II]+	3
6	Rand (1998)	NGC 891	$\parallel$	[O I], [N II], [S II]	45
			$\perp$	[O III], [O I], [N II], [S II]	19
7	Galarza, Walterbos, & Braun (1999)	M31	DIG, SBRs	[O II], [O III], [N II], [S II]+, EM	30
8	Hoopes, Walterbos, & Rand (1999)	NGC 4631	$\perp$	[O III], [S II]+, EM	31
9	Tüllmann & Dettmar (2000)	NGC 1963	$\perp$	[O III], He I, [O I], [N II], [S II], EM	40
		NGC 3044	$\perp$	[O III], He I, [O I], [N II], [S II], EM	47
		NGC 4402	$\perp$	[N II], [S II], EM	24
		NGC 4634	$\perp$	[N II], [S II], EM	40
10	Collins & Rand (2001)	NGC 4302	$\perp$	[N II], [S II]+	13
		NGC 5775	$\perp$	[O I], [O III], [N II], [S II]+	31
		UGC 10288	$\perp$	[O I], [O III], [N II], [S II]+	19
12	Otte, Gallagher, & Reynolds (2002)	NGC 5775	$\perp$	[O II], [O III], [N II], [S II]+	38
		NGC 4634	$\perp$	[O II], [O III], [N II], [S II]+	34
			$\parallel$	[O II], [O III], [N II], [S II]+	32
		NGC 4631	$\parallel$	[O II], [O III], [N II], [S II]+	34
		NGC 3079	$\parallel$	[O II], [O III], [N II], [S II]	53
		NGC 891	$\parallel$	[O II], [N II], [S II]+	50
13	Hoopes & Walterbos (2003)	M33	Interarm	[O III], He I, [N II], [S II], EM	37
		M51	Interarm	[O III], [N II], [S II], EM	26
		M81	Interarm	[O III], [N II], [S II]	2
14	Miller & Veilleux (2003)	UGC 2092	$\perp$	[N II], [S II]	4
		UGC 3326	$\perp$	[N II], [S II]	6
		UGC 4278	$\perp$	[O III], He I, [O I], [N II], [S II]	13
		NGC 2820	$\perp$	[O III], He I, [O I], [N II], [S II]	13
		NGC 3628	$\perp$	[O III], [N II], [S II]	13
		NGC 4013	$\perp$	[O III], He I, [O I], [N II], [S II]	9
		NGC 4217	$\perp$	[O III], [O I], [N II], [S II]	17
		NGC 4302	$\perp$	[O III], He I, [O I], [N II], [S II]	9
		NGC 5777	$\perp$	[O III], [N II], [S II]	6
15	Hidalgo-Gámez (2006)	ESO245-G05	DIG, H II	[O II], [O III], [N II], [S II]	7
		Gr8	DIG, H II	[O III], He I, [N II], [S II]	19
16	Voges & Walterbos (2006)	M33	DIG	[O III], [O I], [N II], [S II]	7
17	Voges (2006)	NGC 891	$\parallel$	[O III], [O I], [N II], [S II], EM	16
			$\perp$	[O III], [O I], [N II], [S II], EM	10
18	Hidalgo-Gámez (2007)	DDO53	DIG, H II	[O III], [S II]	26

[a]These numbers also serve as bibliographical entries in DIGEDA.

[b]Slit orientation in each galaxy. The symbols and descriptors are described in § 2.1.

[c]The line wavelengths are the following: [O II]λ3727, [O III]λ5007, He Iλ5876, [O I]λ6300, [N II]λ6583, [S II]λ6716 and [S II]λ6716 + λ6731.

measurement data sets. Table 1 also summarizes the main characteristics of the observations contained in each reference. The table is structured as follows: Column 1 attributes a unique identification number to each reference, which is later used as a reference label in DIGEDA (Ref_ID), Column 2 contains the bibliographic references, Column 3 lists the names of the galaxies studied in each reference, Column 4 is the slit orientation with respect to the galactic plane in the case of edge-on galaxies: parallel ($\parallel$) or perpendicular ($\perp$), while for the case of face-on galaxies, a short descriptor of the region is used instead:

TABLE 2

COLUMN HEADERS IN DIGEDA[a]

Column	0	1	2	3	4
Information	Obs_ID	Position	[O II] λ3727	[O III] λ4363	Hβ
Column	5	6	7	8	9
Information	[O III] λ4959	[O III] λ5007	He I λ5876	[O I] λ6300	[N II] λ6548
Column	10	11	12	13	14
Information	Hα	[N II] λ6583	[S II] λ6716	[S II] λ6731	[S II] λ6716+6731
Column	15	16	17	18	19
Information	T_e (10^4 K)	[S II] λ6716/6731	[O III] λ5007/4959	Hα/Hβ	EM
Column	20	21	22	23	24
Information	Ref_ID	Morphology	Slit	Region_ID	Gal_ID

[a]See § 2.1 for further details about the information contained in the various entries.

Interarm, DIG (Diffuse Ionized Gas), H II (H II region), SBR (Super Bubble Remnant). In Column 5, we detail the set of emission lines reported for each galaxy while in Column 6 we give the total number of areas or positions[2] observed within each galaxy. There are two factors that may affect the accuracy of the line ratios: dust reddening and the presence of underlying absorption lines. We have not performed any reddening correction although we did use the reddening-corrected ratios when made available by the authors. In any case, all line ratios considered in this Paper involve lines that are relatively close in wavelengths and are therefore not very sensitive to reddening. As for the presence of underlying absorption lines, this is a concern only for Hα and Hβ. The equivalent width of either absorption line is estimated to be ~ -2 Å (Antonio Peimbert, private communication). Since the emission line equivalent widths are *not* available from the works cited in Table 1, we could not correct the ratios for this effect nor evaluate precisely its impact. Further details about the data reduction performed by each author can be found in the corresponding bibliographical entry listed in Table 1. Hereafter, we will consider the symbols [N II], [O I], [O III], [S II], and [S II]+, as referring to the [N II]λ6583, [O I]λ6300, [O III]λ5007, [S II]λ6716 and [S II]λ6716+λ6731 emission lines, respectively.

The 1061 observations obtained from these references were extracted by digitalization of published figures or tables. The data were subsequently normalized and incorporated in DIGEDA. This resulted in a table of 25 comma-separated columns (csv format) containing 1061 data lines (or records).

Missing entries are represented by (-1) in the corresponding data field. The table begins with a header line, which attributes a descriptor to each column. The first column attributes a unique identifying number (Obs_ID) to the observation it refers to. Apart from line ratios or fluxes, additional columns (20 to 25) are provided that describe the particularities of the observation (observed position, slit orientation, ...). The entries contained in these columns consist of numbers (or pointers), which refer to specifically coded information (see description below). This ensures that the information it contains can be easily accessed by any numerical program. A list of all the column headers and the type of information they contain is provided in Table 2.

As we mentioned above, the entries in some of the columns have a numerical format that deserves further clarification: "Obs_ID" is the positive, consecutive and unique number for row identification. "Position" is the value in kpc of the position within each galaxy. In case the observations was carried out perpendicular to the galaxy plane, this is the distance from the plane, for parallel slits this is the position from the galaxy center and for face-on galaxies the position is determined with respect to some reference point that the authors had specified. The ratio Hα/Hβ is that reported by the authors. However, in cases where no value was reported, a theoretical ratio of 2.86 was assumed when its value was required to normalize the forbidden lines. The "EM" is the Hα emission measure, specified in units of pc cm^{-6}. "Ref_ID" is the integer descriptor that identifies the bibliographical reference (see Table 1). "Morphology" refers to the galaxy's morphology and its orientation, as follows: for spiral galaxies 11 is reserved for edge-on objects and 12 for face-on ones;

---

[2]Throughout the paper, we also refer to these positions as "regions".

TABLE 3

LIST OF GALAXIES CONTAINED IN DIGEDA

Gal_ID[a]	Galaxy	R.A.	DEC.	Morphology Type	Inclination
		(h m s)	(d m s)		(degrees)
1	M 31	00 42 44.3	+41 16 09	Sb, LINER	77.5
2	M 33	01 33 50.9	+30 39 36	Scd, H II	56
3	M 51	13 29 55.7	+47 13 53	Sbc	64
4	M 81	09 55 33.2	+69 03 55	Sab;LINER Sy1.8	58
5	M 101	14 03 12.6	+54 20 57	SBcd	17
20	NGC 891	02 22 33.4	+42 20 57	Sb, H II	64
21	NGC 1569	04 30 49.0	+64 50 53	Irr	
22	NGC 1963	05 32 16.8	−36 23 55	Scd	85
23	NGC 2403	07 36 51.4	+65 36 09	SBcd, H II	62
24	NGC 2820	09 21 45.6	+64 15 29	SBc	90
25	NGC 3044	09 53 40.9	+01 34 47	SBb	84
26	NGC 3079	10 01 57.8	+55 40 47	SBc, LINER, Sy 2	60
27	NGC 3628	11 20 17.0	+13 35 23	Sb	87
28	NGC 4013	11 58 31.4	+43 56 48	Sb, H IILINER	90
29	NGC 4217	12 15 50.9	+47 05 30	Sb	86
30	NGC 4302	12 21 42.5	+14 35 54	Sc	90
31	NGC 4395	12 25 48.8	+33 32 49	Sm, LINER, Sy 1.8	38
32	NGC 4402	12 26 07.5	+13 06 46	Sb	74
33	NGC 4631	12 42 08.0	+32 32 29	SBb	85
34	NGC 4634	12 42 40.9	+14 17 45	Sc	83
35	NGC 5775	14 53 57.6	+03 32 40	Sb	86
36	NGC 5777	14 51 17.8	+58 58 41	Sb	83
70	UGC 2092	02 36 31.6	+07 18 34	Scd	86
71	UGC 3326	05 39 37.1	+77 18 45	Scd	90
72	UGC 4278	08 13 58.9	+45 44 32	SBd	90
73	UGC 10288	16 14 24.8	−00 12 27	Sc	87
90	ESO245 - G05	01 45 03.7	−43 35 53	Irr	
91	Gr 8	12 58 40.4	+14 13 03	Irr	
92	DDO 53	08 34 07.2	+66 10 54	Irr	

[a]Unique galaxy identification number within DIGEDA.

2 is used for irregulars. "Slit" is the slit orientation with respect to the galactic plane: 1 for parallel slits, 2 for perpendicular slits and 3 for observations of face-on objects. "Region_ID" refers to the three possible emission region types: 1 and 11 are used for H II regions, 2 and 21 for transition zones, 3 and 31 for DIG regions, and finally, 4 is reserved for data that do not fit any classification. Single digit entries denote the authors original classification (when it was reported) while double digit entries denote our own classification taking into account the value of the height above the galactic plane $|z|$ as described below in § 2.2. Finally, "Gal_ID" is an integer number that relates uniquely the galaxy's name to its source catalog, as follows: Messier: 1–19, New General Catalog: 20–69, Uppsala General Catalog: 70–89 and others: 90–99. The list of all the galaxies in DIGEDA, with their basic characteristics, is given in Table 3.

To sum up, DIGEDA contains 1061 spectroscopic observations. It is worth noting, however, that only 114 observations contain simultaneous measurements of [N II], [O III], [S II] and the EM (these turn out to be edge-on spiral galaxies). But if we consider instead a single pair of lines, for example [N II] and [O III], the number of available data entries in this case increases to 462 observations.

DIGEDA will be made available on-line, at the VizieR website (http://vizier.u-strasbg.fr).

2.2. An additional grouping criterion: $|z|$

Due to the fact that there is no standard criterion to distinguish DIGs from H II regions, most of the authors in the field report their spectroscopic studies without any classification. For instance, $\simeq 76\%$ of the 1061 observations in the DIGEDA are neither referred to as H II region, DIG or transition zone.

About $\sim 97\%$ of these data correspond to edge-on galaxy observations, which are of particular interest among diffuse ionized gas studies. For this galaxy type, the halo gas is easier to separate from the disk (where most H II regions are located). In that case, the DIG emission can be reasonably assumed to be free from contamination by star formation emission. Considering that in the Milky Way, the thin disk is defined as the region where most of the galaxy's star formation is taking place, we propose in this Paper a 'zoning' classification criterion based on the height (above or below) the galactic plane $|z|$. The proposed zoning classification leads to the following three situations:

- $|z| < 500\,\mathrm{pc}$. Owing to the fact that in the Milky Way, one considers that H II regions are confined to a disk of $350\,\mathrm{pc}$ height, we have assumed this to be a general behavior in spiral galaxies. We will therefore consider that line emission from regions within $500\,\mathrm{pc}$ from the galactic plane corresponds overwhelmingly to emission from star forming regions. Consequently, we will classify these regions as *H II regions* ("Region_ID"=11).

- $500 \leq |z| < 1000\,\mathrm{pc}$. The majority of spiral galaxies from the database do not have an inclination of exactly $90°$ and it is therefore probable that, due to projection effects, a line of sight below or above the galactic plane of between 500 and 1000 pc will cross a large volume, which likely will contain both DIG and H II region emission. Since we do not know precisely the contribution from each type, we will classify these regions as being from *transition zones* ("Region_ID"=21).

- $|z| \geq 1\,\mathrm{kpc}$. Even though some authors have reported the existence of H II regions as far away as $1.5\,\mathrm{kpc}$ from the plane, this remains an uncommon occurrence. In this work, we will assume that the emission from any lines of sight above $|z| = 1\,\mathrm{kpc}$ from the galactic plane is free from any contamination from star formation emission. This leads us to classify these regions as *eDIG* ("Region_ID"=31).

Applying this 'zoning' classification to the database resulted in 309 H II regions, 218 transition zones, and 509 eDIGs. Only 2% of the observations could not be classified. They turn out to come from face-on galaxies where our criterion based on $|z|$ is not applicable.

3. ANALYSIS AND INTERPRETATION OF THE DIGEDA DATA

We have carried out a statistical study of the database with the aim of identifying the main differences between DIGs and H II regions. To assist us, we used the line ratio diagnostic diagrams prescribed by Baldwin, Phillips, & Terlevich (1981) and by Veilleux & Osterbrock (1987). Such diagrams were created with the intention of classifying line emitting regions according to their physical conditions, yet using only the most commonly measured lines, that is: Hα, Hβ, [N II], [O I], [O III], and [S II]. Baldwin et al. (1981)[3] and Veilleux & Osterbrock (1987) found that these diagrams provide a quantitative classification scheme of extragalactic sources, in which the main excitation mechanism operating on the gas is identified, namely: photoionization by O and B stars, photoionization by a power-law continuum source, shock-wave heating and photoionization by old and very hot stars. Apart from being used for the above purpose, these diagrams also turn out to be useful in other situations or for other kinds of emission objects (e.g., distinguishing planetary nebulae from H II regions, see Kniazev, Pustilnik, & Zucker 2008). Since the emission lines quoted above are among the most commonly observed lines in DIG regions as well, we adopted the line-ratio diagnostic diagrams in our statistical study.

3.1. *Results from line ratio diagnostic diagrams*

In Figures 1 and 2, we show, for the whole database, the line ratios [O III]/Hβ, [O I]/Hα, [S II]/Hα, and [S II]+/Hα as a function of the ratio [N II]/Hα. Figure 1 distinguishes the different galaxy types as follows: Irregular galaxies (asterisks), spiral face-on galaxies (triangles) and edge-on spirals (squares). Figure 2, which is discussed below, distinguishes among the three emission region types defined in § 2.1.

Our Panel (a) in Figure 1 shows that the data describes a "seagull" shape quite similar to that found by Stasińska et al. (2006) from a study of 20,000 "normal" star-forming and AGN galaxies extracted from the SLOAN database. While the line ratios from both spiral types (edge-on and face-on) extend over the full seagull area in Panel (a) of Figure 1, those from irregular galaxies tend to occupy only the extreme left wing (lower [N II]/Hα and greater [O III]/Hβ values). In the other Panels (b), (c) and (d) of Figure 1, the same remarkable behavior is

---

[3]Hereafter, we will refer to the [N II]/Hα vs. [O III]/Hβ diagram as 'BPT diagram'.
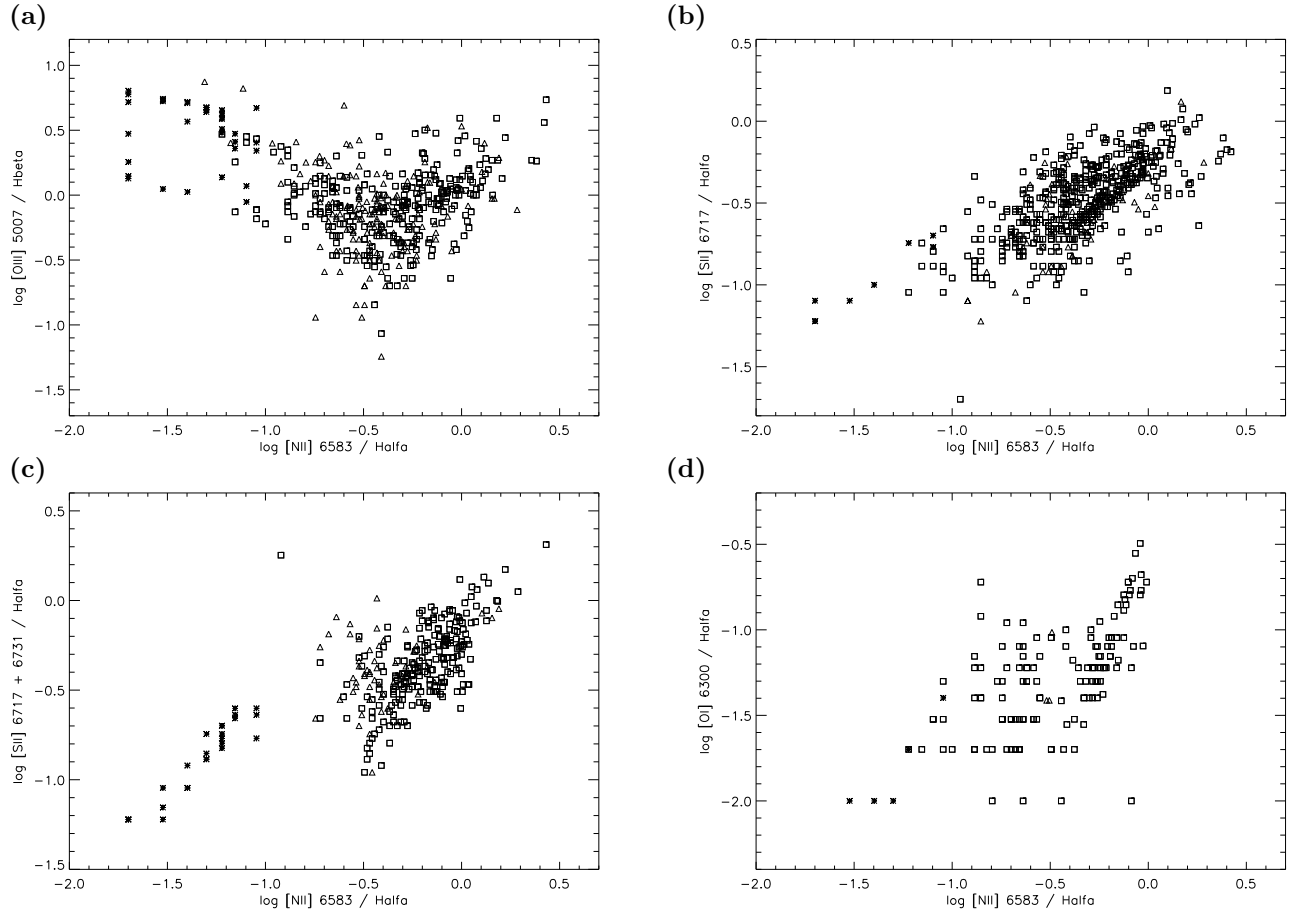
(a)

(b)

(c)

(d)

Fig. 1. Diagnostic diagrams for all observations in the database. The data points identify the galaxy types as follows: irregular galaxies (asterisks), face-on spiral galaxies (triangles), and edge-on spiral galaxies (squares).

found. Notwithstanding the reasons for such behavior (see § 4), it is statistically apparent that the data from irregular and spiral galaxies should not be analyzed without differentiating the galactic type. Since DIGEDA contains only nine observations of irregular galaxies, we chose to consider only spiral galaxies in the analysis that follows.

Figure 2 is similar to the previous figure, except that it distinguishes among the three types of emission line regions: H II regions (blue diamonds), transition zones (green crosses) and DIGs (red pluses). In Panel (a), DIGs and H II regions conform together a "seagull" shape. However, it becomes evident in this BPT diagram that the DIGs occupy a very different location with respect to the H II regions. While H II regions are principally located in the left seagull wing, DIGs cover the right seagull wing, i.e. the two types can be distinguished from their [N II]/Hα ratio alone.

Although less apparent, we can see in Panels (b) and (c) of Figure 2 that DIGs tend furthermore to

have [S II]/Hα ratios greater than those from H II regions. This behavior has been previously mentioned on several occasions (Bland-Hawthorn et al. 1991a; Zurita et al. 2000; Rand 1998; Haffner, Reynolds, & Tufte 1999; Tüllmann & Dettmar 2000) for different galaxies using different classification criteria. The importance of this figure in DIG studies is that it makes clear that even when the data have been classified using a very different criterion, the intensities of [N II] and [S II] are significantly greater in general in DIGs than in H II regions. Perhaps the spread in position of each type and the extent to which they overlap (which differ in each panel) could also be the manifestation of the absence of an universally accepted classification scheme to distinguish the emission region type.

Conspicuously, Panel (d) of Figure 2 does not show any clear trend in the behaviour of the [O I]/Hα line ratio. The data dispersion and the overlap in this panel are both larger than found with [N II] or [S II], possibly because the [O I] line is the weakest

of all lines considered here. In this case, we can expect the [O I] measurements to be more difficult and uncertain, which is consistent with the fact that we only have 148 [O I] measurements (all types together) available among the 1061 observations.

3.2. *The [N II]/Hα line ratio criterion*

Even though our diagnostic diagrams in Figure 2 strongly suggest the existence of a clear separation between H II regions and DIGs in the behavior of [N II]/Hα and [S II]/Hα, a significant overlap is nevertheless present. It thus becomes essential to make a quantitative comparison of the distributions of the various line ratios. This exercise would allow us to identify which ratios show the most significant differences between DIGs and H II regions in the distribution of their values. For this purpose, we can use box diagrams, which summarize in a very schematic fashion the intrinsic distribution of any of the data entries. In such diagrams, each box contains 50% of the data and each has been defined using quartiles Q1 and Q3, which are the lowest and highest 25% cuts-offs in the data distribution. In such boxes, a vertical line denotes the position of the median of the distribution, while "whiskers" are used to represent distribution boundaries that include 80% of the data, which have been defined using the deciles D1 and D9, corresponding to the lowest and highest 10% cut-offs.

Figure 3 shows such box diagrams for the EM values and for each of the most prominent line ratios (from spiral galaxies) contained in DIGEDA. Each datum's statistic distinguishes whether it considers only DIGs or H II regions, using the label (D) or (H), respectively. It is apparent that a few conspicuous line ratios show a distribution that is significantly *distinct* between DIGs and H II regions. These ratios correspond to those boxes that do not overlap (or overlap slightly) in log (I) position when comparing the (D) and (H) boxes of the same quantity. It is also obvious that, conversely, many line ratios show an important overlap in the position of the (D) and (H) boxes.

If we consider the line ratios of [O I], [S II], [S II]+ and [N II] with respect to Hα, the following sample sizes are available: [O I] (157 entries), [S II] (521 entries), [S II]+ (322 entries) and [N II] (888 entries). It is noteworthy that for each of these 4 line ratios, the distributions that the boxes in Figure 3 represent do *not* overlap between the (D) and (H) entries. That is, these 4 line ratios show clear differences in their quantiles distribution between DIGs and H II regions. This quantitative analysis gives us further

confidence in proposing that a few line ratios are by themselves sufficient to empirically distinguish a DIG region from an H II region, notwithstanding the lack of any prior knowledge about the electron density or column size (both quantities being unknown in DIGs).

Even considering that any of the above four lines ratios could be a useful criterion for distinguishing DIGs, the [N II]/Hα statistic corresponds to the largest data sample. Observationally, it is also perhaps the ratio that is easiest to measure (since [N II] is a strong line and the [N II]/Hα ratio does not require any reddening correction).

In Table 4, the numerical values of the different quantiles for [N II]/Hα are sumarized. It can be concluded that emission regions with [N II]/Hα < -0.5 should be classified as H II regions, while those with [N II]/Hα > -0.3 should be classified as DIGs. Measurements of intermediate values result in an uncertain classification. In any case, we can infer that emission regions with a ratio [N II]/Hα < -0.4 have a high probability of being an H II region while regions with [N II]/Hα > -0.4 have a higher probability of being a DIG.

Additionally, the boxes in Figure 3 representing the ratios [O III]/Hβ, [N II]/[S II], [N II]/[S II]+, and [N II]/[O III] do *not* show a significant difference in distribution between DIGs and H II regions. These ratios are therefore useless for distinguishing one type of region from another.

Some authors have proposed to use the EM as a classification criterion (e.g., Walterbos & Braun 1994). We note, however, from Figure 3 that the box diagrams of EM do not show any significant differences between the DIG and H II region distributions. Other authors (e.g., Bland-Hawthorn et al. 1991a,b; Rand 1998) have suggested that the [N II]/Hα ratio shows a strong anti-correlation with the EM, i.e. the [N II]/Hα would increase as the EM decreases. To which extent therefore can the EM be a distinguishing universal criterion for DIGs? Even though the EM distribution box in Figure 3 suggests that we cannot (because of a large overlap of the (D) and (H) boxes), we may nevertheless consider the possibility that within a single galaxy, this criterion might be applicable. After all, it is the only quantity in the box diagrams of Figure 3 that does not correspond to a ratio and is therefore not normalized. The wide overlap might for instance be the result of a wide spread in EM values from galaxy to galaxy.

In order to explore further this question, we plotted EM values against several emission line ratios. As expected, we found a very feeble general rela-

tionship and only in the case of [N II]/Hα. However, when we considered individual galaxies separately, a different picture emerged. Our results are summarized in Figure 4 where Panel (a) has [N II]/Hα in the abscissa and Panel (b) [O III]/Hβ, while the EM is displayed in the ordinate. A different color coding is used for each galaxy: M33 (magenta), M51 (cyan), NGC 1963 (yellow), NGC 3044 (red), NGC 4402 (green), NGC 891 (black), NGC 4634 (blue, Panel (a) only), NGC 4631 (blue, Panel (b) only). The best log-log fits of the points of each galaxy are overplotted. In Panel (a), we see that there exists indeed a relationship between EM and [N II]/Hα for each galaxy *individually*. In the case of [O III]/Hβ (Panel b), a similar but weaker relationship appears to be present as well.

Even though a general EM-based criterion cannot be defined (Figure 3), it is apparent from Figure 4 that when the [N II]/Hα ratio (Table 4) is used to determine the emission region type, a critical value EM_c can then be found that appears to be different for each galaxy individually. We obtain the interesting result that emission regions with $EM > EM_c$ can be considered to be H II regions while emission regions *in the same galaxy* with $EM < EM_c$ turn out to be DIGs. This particular EM_c criterion, defined for each galaxy, is based on the more general [N II]/Hα criterion. EM_c allows us now to distinguish DIGs from H II regions with certainty, confirming that the basic physical conditions (as represented by line ratios) in these two region types are indeed different.

4. DISCUSSION

Following our statistical analysis of the database, there are two results that deserve further discussion: on the one hand, the different physical conditions taking place in DIGs and H II regions (in the context of spiral galaxies) and, on the other hand, the extreme position that the DIGs from irregular galaxies occupy in the BPT-diagram with respect to the DIGs from spirals.

4.1. *DIG and H II regions: what is the underlying difference?*

BPT proposed a way to classify emission line regions, which is based on their location in the [O III]/Hβ vs. [N II]/Hα diagnostic diagram. These authors were successful in separating H II regions (low [N II]/Hα) from LINERS and Seyfert galaxies (high [N II]/Hα). Using data from DIGEDA, we found that most of the DIGs fall in the regions occupied by LINERS and Seyferts (see Figure 2). However, we cannot foresee how in non-active galaxies

the same kind of photoionization source that powers AGN could replace O–B stars of H II regions and become responsible for the excitation of the DIG.

More recently, using the SDSS survey Stasińska et al. (2008) proposed an original interpetation for objects occupying the right part of the BPT diagram (which they dubbed the seagull's right wing). They pointed out that the simultaneous increase of [O III]/Hβ and [N II]/Hα can also be the result of photoionization by hot old stars, for example the central stars of planetary nebulae (PNe). According to this interpretation, the ionizing source of the DIG would be similar to that of H II regions (i.e. a stellar continuum), except for the effective temperature of the ionizing stars and, consequently, the higher electron temperature of the gas.

Following the conclusions reached by Stasińska et al. (2008), we propose that the DIG could be ionized by old stars, at least in spiral galaxies. In fact, the suggestion that a hot stellar population might contribute to the ionizing source was first proposed by Lyon (1975) and later explored by Sokolowski & Bland-Hawthorn (1991) who developed photoionization models that combine OB stars with old hot stars. Sokolowski & Bland-Hawthorn (1991) concluded that such composite models can reproduce the DIGs observations in NGC 891. However, as early as in 1991, the available observational data were scant and no [O III]/Hβ ratios from DIGs had yet been published.

One can find other explanations for the position of DIGs in the BPT diagram besides that of a hotter photoionization source. For instance, the photoionization models developed by Sokolowski (1993) suggest that the ionizing flux from O and B stars could simulate the effect of a hotter source when intervening dust is present (between the stars and the DIG) and the selective extinction by such dust is taken into account. A similar UV hardening could also result from the radiation that leaks out from disk H II regions (Domgorgen & Mathis 1994; Zurita et al. 2000). Both effects of selective absorption and of photoionization by old and hot stars are the subject of a paper in preparation.

4.2. *DIG in irregular galaxies*

The DIGs observed in irregulars occupy the same part of the BPT-diagram as do the H II regions of spiral galaxies (low [N II]/Hα in Figure 1). Furthermore, we have no evidence of any DIG from irregulars occupying the high [N II]/Hα part of the diagram. About the first aspect mentioned above (low [N II]/Hα), given the fact that the position of

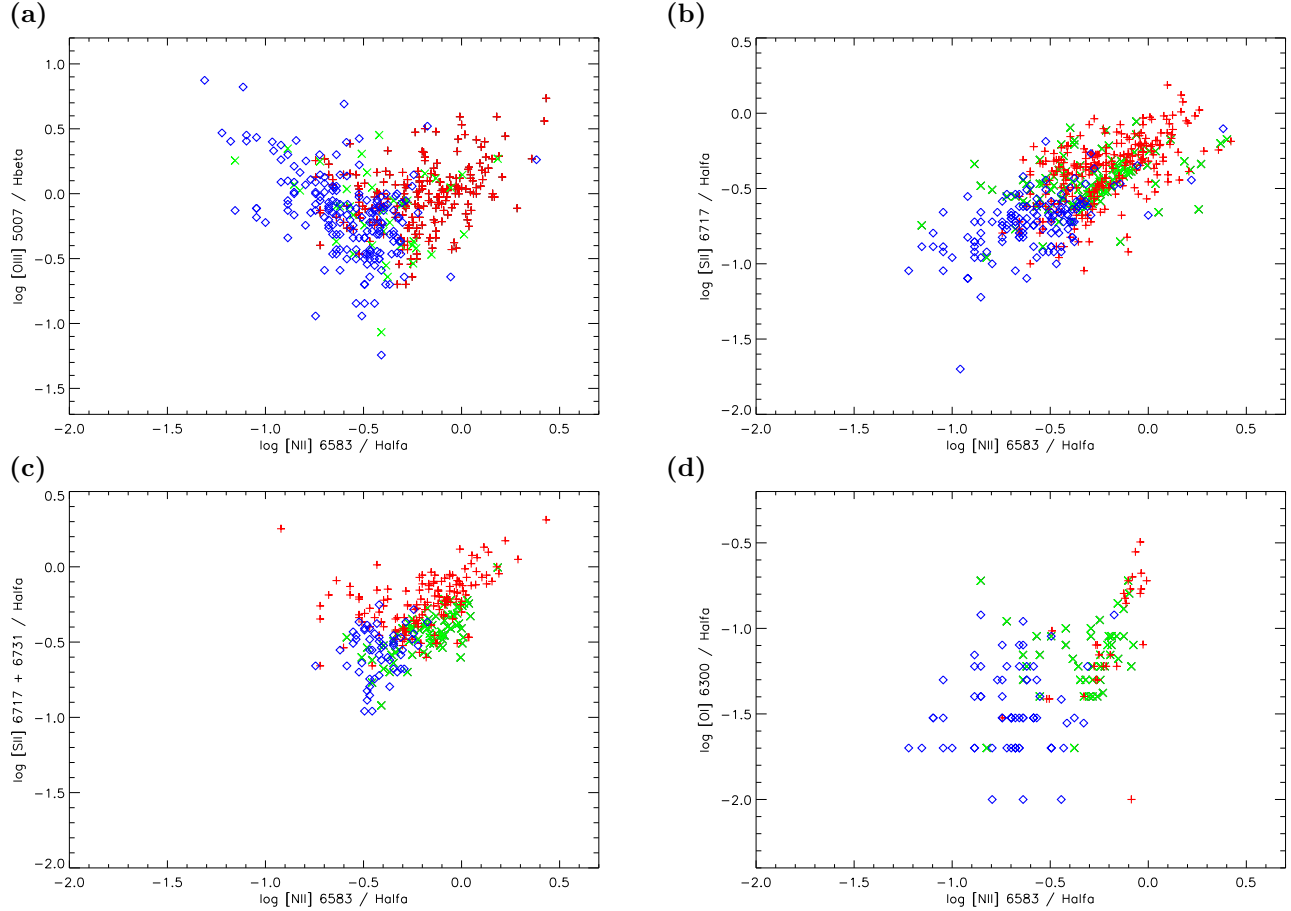**(a)**

(b)

(c)

(d)

Fig. 2. Diagnostic diagrams for all observations in the database. The data points identify the emission region types as follows: H II regions (blue diamonds), transition zones (green crosses) and DIGs (red pluses).

an emission line object in the BPT diagram is related to specific physical conditions of the gas, our results suggest that the so-called DIG from irregular galaxies could in fact just be the manifestation of low surface brightness H II regions.

On the other hand, the lack of DIG from irregulars at high [N II]/Hα could have several alternative explanations. First, it could be that this emission is too weak to have been detected yet. Another possible explanation follows from the idea developed in the previous section, namely, that the DIG ionization results from "old stars". It is conceivable that in irregular galaxies the old stellar population is proportionally much smaller than in spiral galaxies, the effect of which would be that this population could not then contribute significantly to the ionization budget. In any event, since we only have a few data points in the case of irregular galaxies (7 H II regions and only 2 DIGs with measurements of [N II] and [O III]), we cannot yet reach definitive conclusions about irregulars.

TABLE 4

QUANTIL VALUES FOR [N II]/Hα

	D1	Q1	Median	Q3	D9
H II reg	−0.89	−0.68	−0.52	−0.41	−0.33
DIG	−0.51	−0.38	−0.22	−0.04	0.09

5. CONCLUSIONS

In this work, we present the first emission line database from DIGs (DIGEDA) made up from spectroscopic data available in the literature. The database is a compilation of 17 bibliographical references. It contains 1061 observed regions (309 H II regions, 218 transition zones and 509 DIGs) out of 29 galaxies (spirals and irregulars) and is freely available from CDS.

DIGEDA has allowed us to carry out for the first time a statistical analysis that aimed at characterizing the general behavior of the strongest emission lines, and at finding global trends among the vari-
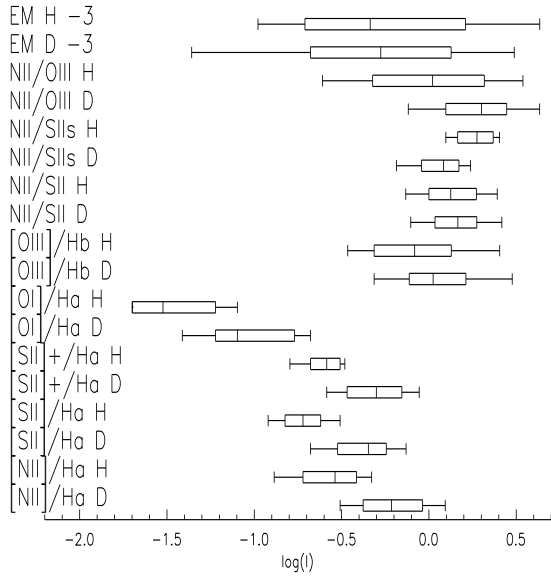
Fig. 3. Box diagrams of the data distributions of the EM and of the most prominent line ratios from DIGs and H II regions (D and H labels, respectively). All the values are logarithmic, with that of the EM reduced by 3 dex.

Fig. 4. The EM against (a) [N II]/Hα and (b) [O III]/β. A different color coding is used for each galaxy: M33 (magenta), M51 (cyan), NGC 1963 (yellow), NGC 3044 (red), NGC 4402 (green), NGC 891 (black) and NGC 4634 (blue, in panel a), NGC 4631 (blue, in panel b). The best log-log linear fits of the points of each galaxy are overplotted using the same color coding.

ous line ratios, including the EM. One of the results is that the DIGs of irregular galaxies show extreme values in their line ratios with respect to that of spirals (see § 3 and § 4). These, in fact, lie close to the values observed in H II regions. Since the available data are very limited, it is indispensable to obtain more observations to confirm this result.

The analysis carried out with DIGEDA leads us to define a universal criterion for spiral galaxies, which allows distinguishing DIGs from H II regions. The distribution of [N II]/Hα ratios shows that [N II]/Hα = −0.4 defines a critical value: any emission region with a ratio greater than −0.3 should be classified as DIG while a ratio below −0.5 is likely to come from an H II region.

Taking advantage of the high number of data in DIGEDA, we could confirm (or refute) the reality of line ratio behaviors that have been proposed in the literature concerning individual galaxies. We could check to what extent these applied to all DIGs taken together. This is the case for the [N II]/Hα ratio, which shows a well defined anti-correlation with EM, but of varying slopes between galaxies. These variations in the log-log slopes rule out any definition of a universal EM value to distinguish DIGs from H II regions. Nevertheless, a critical value, EM_c, can be defined for each galaxy individually.

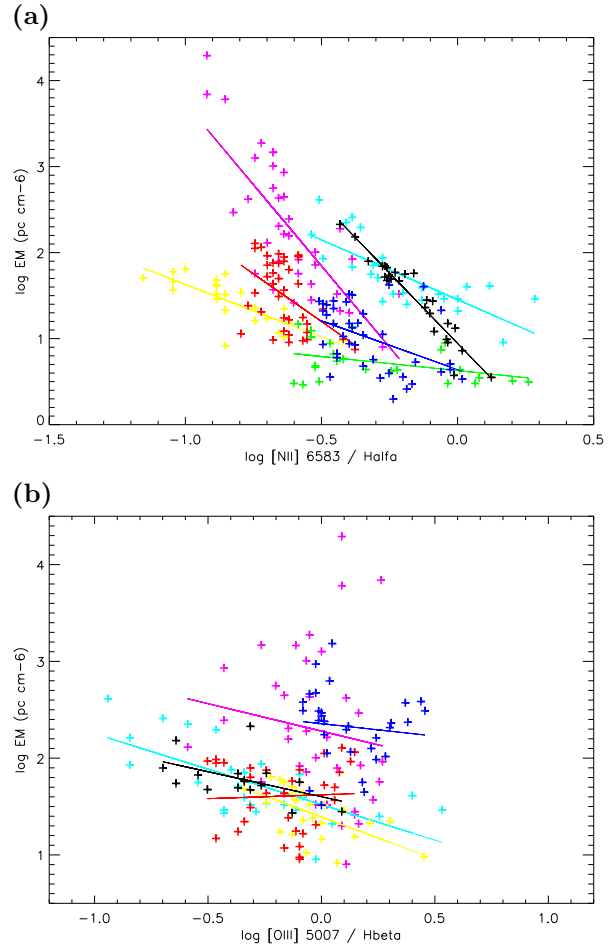## REFERENCES

Baldwin, J. A., Phillips, M. M., & Terlevich, R. 1981, PASP, 93, 5 (BPT)

Benvenuti, P., D'Odorico, S., & Peimbert, M. 1976, RevMexAA, 2, 3

Binette, L., Flores-Fajardo, N., Raga, A. C., Drissen, L., & Morisset, C. 2009, ApJ, 695, 552

Bland-Hawthorn, J., Freeman, K. C., & Quinn, P. J. 1997, ApJ, 490, 143

Bland-Hawthorn, J., Sokolowski, J., & Cecil, G. 1991a, PASP, 103, 906

_____. 1991b, ApJ, 375, 78

Collins, J. A., & Rand, R. J. 2001, ApJ, 551, 57

Dettmar, R. J. 1990, A&A, 232, L15

Dettmar, R. J., & Schultz, H. 1992, A&A, 254, L25

Domgorgen, H., & Mathis, J. S. 1994, ApJ, 428, 647

Ferguson, A. M. N., Wyse, R. F. G., Gallagher, III., J. S., & Hunter, D. A. 1996, AJ, 111, 2265

Galarza, V. C., Walterbos, R. A. M., & Braun, R. 1999, AJ, 118, 2775

Golla, G., Dettmar, R. J., & Domgorgen, H. 1996, A&A, 313, 439

Greenawalt, B., Walterbos, R. A. M., & Braun, R. 1997, ApJ, 483, 666

Haffner, L. M., Reynolds, R. J., & Tufte, S. L. 1999, ApJ, 523, 223

Hidalgo-Gámez, A. M. 2006, AJ, 131, 2078

_____. 2007, AJ, 134, 1447

Hoopes, C. G., & Walterbos, R. A. M. 2003, ApJ, 586, 902

Hoopes, C. G., Walterbos, R. A. M., & Rand, R. J. 1999, ApJ, 522, 669

Hoyle, F,. & Ellis, G. R. A. 1963, Australian J. Phys., 16, 1

Kniazev, A. Y., Pustilnik, S. A., & Zucker, D. B. 2008, MNRAS, 384 1045

Lyon, J. 1975, ApJ, 201, 168

Martin, C. L., & Kennicutt, Jr., R. C. 1997, ApJ, 483, 698

Miller, S. T., & Veilleux, S. 2003, ApJS, 148, 383

Otte, B., Gallagher, III, J. S., & Reynolds, R. J. 2002, ApJ, 572, 823

Rand, R. J. 1998, ApJ, 501, 137

Rand, R. J., Wood, K., & Benjamin, R. A. 2009, in The Evolving ISM in the Milky Way and Nearby Galaxies, ed. K. Sheth, A. Noriega-Crespo, J. Ingalls, & R. Paladini (http://ssc.spitzer.caltech.edu/mtgs/ismevol/)

Reynolds, R. J. 1990, ApJ, 349, L17

_____. 1991, in IAU Symp. 144, The Interstellar Disk-Halo Connection in Galaxies, ed. H. Bloemen (Dordrecht: Kluwer), 67

Reynolds, R. J., Scherb, F., & Roesler, F. L. 1973, ApJ, 185, 869

Sivan, J. P., Stasińska, G., & Lequeux, J. 1986, A&A, 158, 279

Sokolowski, J. 1993, in ASP Conf. Ser. 35, Massive Stars: Their Lives in the Interstellar Medium, ed. J. P. Cassinelli, & E. B. Churchwell (San Francisco: ASP), 540

Sokolowski, J., & Bland-Hawthorn, J. 1991, PASP, 103, 911

Stasińska, G., Cid Fernandes, R., Mateus, A., Sodré, L., & Asari, N. V. 2006, MNRAS, 371, 972

Stasińska, G., et al. 2008, MNRAS, 391, L29

Tüllmann, R., & Dettmar, R. J. 2000, A&A, 362, 119

Veilleux, S., Cecil, G., & Bland-Hawthorn, J. 1995, ApJ, 445, 152

Veilleux, S., & Osterbrock, D. E. 1987, ApJS, 63, 295

Voges, E. S. 2006, PhD Thesis, New Mexico State University

Voges, E. S., & Walterbos, R. A. M. 2006, ApJ, 644, L29

Walterbos, R. A. M., & Braun, R. 1994, ApJ, 431, 156

Wang, J., Heckman, T. M., & Lehnert, M. D. 1997, ApJ, 491, 114

Zurita, A., Rozas, M., & Beckman, J. E. 2000, A&A, 363, 9

Luc Binette, Nahiely Flores-Fajardo, and Christophe Morisset: Instituto de Astronomía, Universidad Nacional Autónoma de México, Apdo. Postal 70-264 04510, México D.F., Mexico (nahiely, morisset@astroscu.unam.mx).